



Di-*n*-butylbis[*N*-(2-methoxyethyl)-*N*-methyldithiocarbamato- κ^2 S,*S'*]tin(IV): crystal structure and Hirshfeld surface analysis

Rapidah Mohamad,^a Normah Awang,^{b,‡} Nurul F. Kamaludin,^b Mukesh M. Jotani^c and Edward R. T. Tiekink^{d,*}

Received 19 January 2017

Accepted 22 January 2017

Edited by W. T. A. Harrison, University of Aberdeen, Scotland

‡ Additional correspondence author, e-mail: awang_normah@yahoo.com.

Keywords: crystal structure; organotin; dithiocarbamate; Hirshfeld surface analysis.

CCDC reference: 1528948

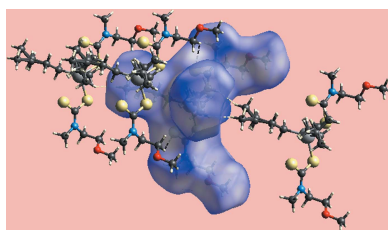
Supporting information: this article has supporting information at journals.iucr.org/e

^aBiomedical Science Programme, School of Diagnostic and Applied Health Sciences, Faculty of Health Sciences, Universiti Kebangsaan Malaysia, Jalan Raja Muda Abdul Aziz, 50300 Kuala Lumpur, Malaysia, ^bEnvironmental Health and Industrial Safety Programme, School of Diagnostic and Applied Health Sciences, Faculty of Health Sciences, Universiti Kebangsaan Malaysia, Jalan Raja Muda Abdul Aziz, 50300 Kuala Lumpur, Malaysia, ^cDepartment of Physics, Bhavan's Sheth R. A. College of Science, Ahmedabad, Gujarat 380 001, India, and ^dResearch Centre for Chemical Crystallography, School of Science and Technology, Sunway University, 47500 Bandar Sunway, Selangor Darul Ehsan, Malaysia. *Correspondence e-mail: edwardt@sunway.edu.my

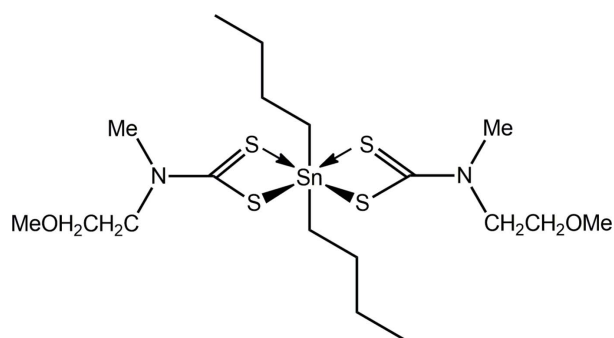
The complete molecule of the title compound, [Sn(C₄H₉)₂(C₅H₁₀NOS₂)₂], is generated by a crystallographic mirror plane, with the Sn^{IV} atom and the two inner methylene C atoms of the butyl ligands lying on the mirror plane; statistical disorder is noted in the two terminal ethyl groups, which deviate from mirror symmetry. The dithiocarbamate ligand coordinates to the metal atom in an asymmetric mode with the resulting C₂S₄ donor set defining a skew trapezoidal bipyramidal geometry; the *n*-butyl groups are disposed to lie over the longer Sn—S bonds. Supramolecular chains aligned along the *a*-axis direction and sustained by methylene-C—H···S(weakly coordinating) interactions feature in the molecular packing. A Hirshfeld surface analysis reveals the dominance of H···H contacts in the crystal.

1. Chemical context

The structural chemistry of molecules with the general formula R₂Sn(S₂CNRR')₂ is diverse with coordination geometries ranging from five, as in trigonal bipyramid (*t*-Bu)₂Sn(S₂CNMe₂)₂ (Kim *et al.*, 1987), to seven, as in pentagonal bipyramidal [MeOC(=O)CH₂CH₂]₂Sn(S₂CNMe)₂ (Ng *et al.*, 1989). However, the overwhelming majority of structures are comprised of a six-coordinate Sn^{IV} atom, being based on either skew trapezoidal bipyramidal or octahedral coordination geometries (Tiekink, 2008). In the former, the dithiocarbamate ligands are coordinating in an asymmetric mode and lie in a plane, with the Sn-bound organic substituents orientated over the weaker Sn—S bonds. In the octahedral molecules, the Sn-bound substituents occupy mutually *cis*-positions. As a general observation, compounds with Sn-bound aryl groups are octahedral and those with Sn-bound alkyl groups are skew trapezoidal bipyramidal. However, the capricious nature of the ultimate structure adopted in the solid state is nicely illustrated in a recent study whereby Ph₂Sn[S₂CN(CH₂CH₂OMe)Me]₂, with a dithiocarbamate ligand with dissimilar substituents, was found to be octahedral but, Ph₂Sn[S₂CN(CH₂CH₂OMe)₂]₂, with the dithiocarbamate ligand having similar substituents, was skew trapezoidal bipyramidal (Mohamad, Awang, Jotani *et al.*, 2016). The structural interest notwithstanding, organotin dithiocarbamates have potential biological applications, with recent



investigations focusing upon biocidal activities, *e.g.* anti-fungal (Yu *et al.*, 2014) and anti-bacterial (Ferreira *et al.*, 2012), and, especially, as anti-cancer agents (Ferreira *et al.*, 2014; Kadu *et al.*, 2015), the focus of our interest (Khan *et al.*, 2014, 2015). During the course of the latter studies, crystals of the title compound, $n\text{-Bu}_2\text{Sn}[\text{S}_2\text{CN}(\text{CH}_2\text{CH}_2\text{OMe})\text{Me}]_2$, (**I**), became available. Herein, the crystal and molecular structures of (**I**) are described along with a detailed analysis of the molecular packing *via* an analysis of the Hirshfeld surface.



1.1. Structural commentary

The asymmetric unit of (**I**) comprises half a molecule being located on a crystallographic mirror plane with the Sn atom along with the two inner C atoms of the *n*-butyl groups lying on the plane, Fig. 1. The dithiocarbamate ligand coordinates the Sn atom in an asymmetric fashion with the $\Delta(\text{Sn}-\text{S})$, *i.e.* the difference between the $\text{Sn}-\text{S}_{\text{long}}$ and $\text{Sn}-\text{S}_{\text{short}}$ distances, being *ca* 0.39 Å, Table 1. This asymmetry is reflected in the associated C–S bond lengths with the short Sn–S bond being correlated with a long C–S bond length, Table 1. The coordination environment is completed by two α -C atoms of the *n*-butyl groups. The four S atoms are co-planar and define

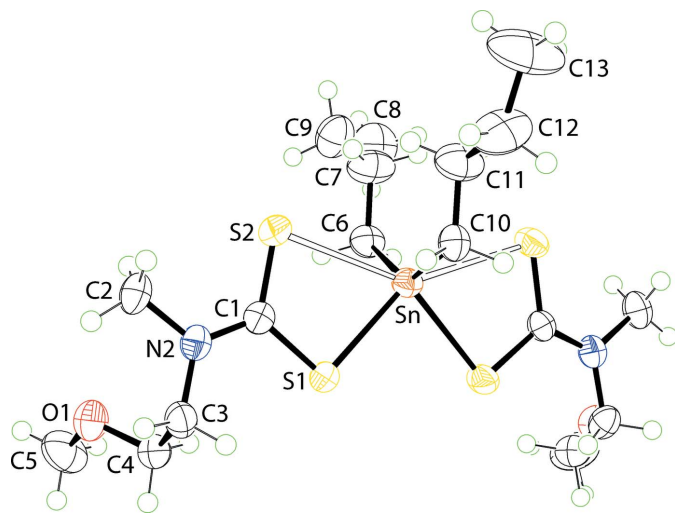


Figure 1

The molecular structure of (**I**), showing the atom-labelling scheme and displacement ellipsoids at the 70% probability level. Unlabelled atoms are related by the symmetry operation $(x, \frac{1}{2} - y, z)$. Only one component of each of the disordered *n*-butyl groups is shown.

Table 1

Selected bond lengths (Å).

Sn–S1	2.5425 (5)	Sn–C10	2.138 (3)
Sn–S2	2.9318 (5)	S1–C1	1.7443 (18)
Sn–C6	2.146 (3)	S2–C1	1.6974 (19)

Table 2

Hydrogen-bond geometry (Å, °).

$D\text{---}H\cdots A$	$D\text{---}H$	$H\cdots A$	$D\cdots A$	$D\text{---}H\cdots A$
$\text{C4---H4B}\cdots\text{S2}^i$	0.99	2.96	3.608 (2)	124

Symmetry code: (i) $x - 1, y, z$.

a skewed trapezoidal plane, and the α -C atoms are disposed over the weaker Sn–S bonds so that the C_2S_4 donor set defines a skew trapezoidal bipyramidal geometry.

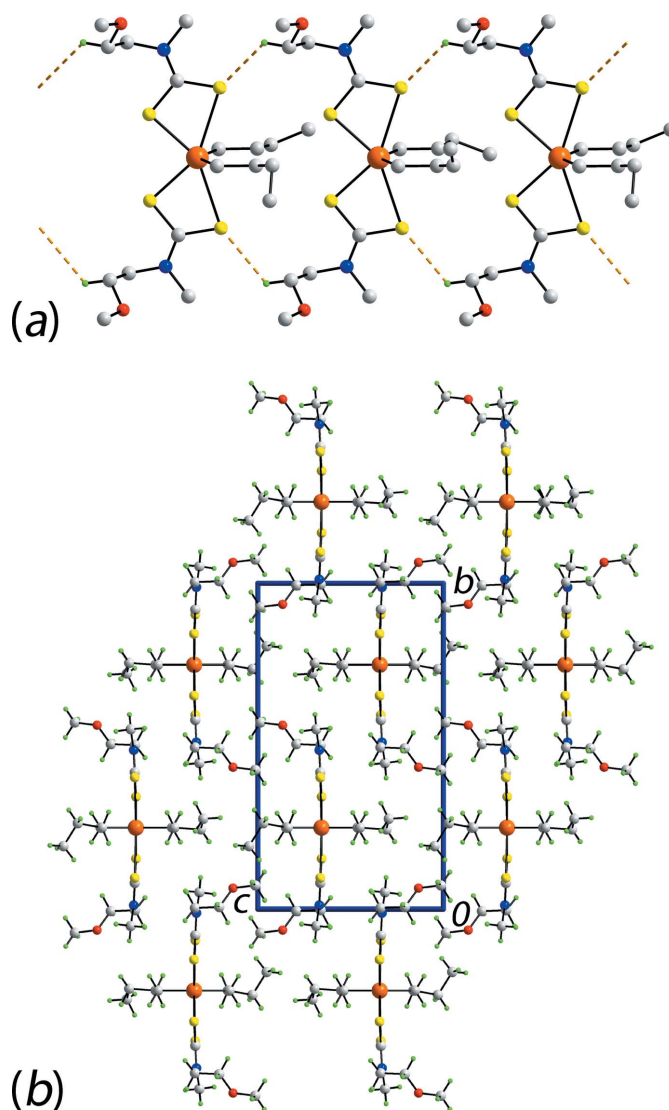


Figure 2

The molecular packing in (**I**): (a) supramolecular chain along the *a* axis sustained by methylene-C–H \cdots S interactions shown as orange dashed lines and (b) a view of the unit cell contents in projection down the *a* axis. Only one component of each of the disordered *n*-butyl groups is shown.

2. Supramolecular features

The only notable contacts identified in the molecular packing are methylene-C—H...S(weakly coordinating) interactions that assemble molecules into linear supramolecular chains propagating along the *a*-axis direction, Fig. 2*a* and Table 2. The chains pack in the crystal with no specific interactions between them, Fig. 2*b*. In order to ascertain more information of the nature of interactions between molecules, the molecular packing and its Hirshfeld surface was analysed, as discussed in *Hirshfeld surface analysis*.

3. Hirshfeld surface analysis

The Hirshfeld surface analysis for (I) was performed as described recently for organotin dithiocarbamates (Mohamad,

Awang, Kamaludin *et al.*, 2016). From the views of the Hirshfeld surface mapped over d_{norm} , in the range -0.298 to $+1.346$ au, in Fig. 3, the pairs of bright-red spots near hydrogen atoms H9C and H13B of the disordered methyl groups, *i.e.* deviating from mirror symmetry, indicate their participation in specific intermolecular H...H interactions. In the crystal, these lead to a supramolecular chain along the *c* axis. The presence of this dihydrogen interaction, resulting from disparate charges on respective hydrogen atoms, can also be viewed by the different curvatures and electrostatic potentials around these atoms on the Hirshfeld surface mapped over the electrostatic potential in the range -0.082 to $+0.163$ au, Fig. 4. Fig. 5 illustrates the immediate environment around a reference molecule within its Hirshfeld surface mapped over d_{norm} ,

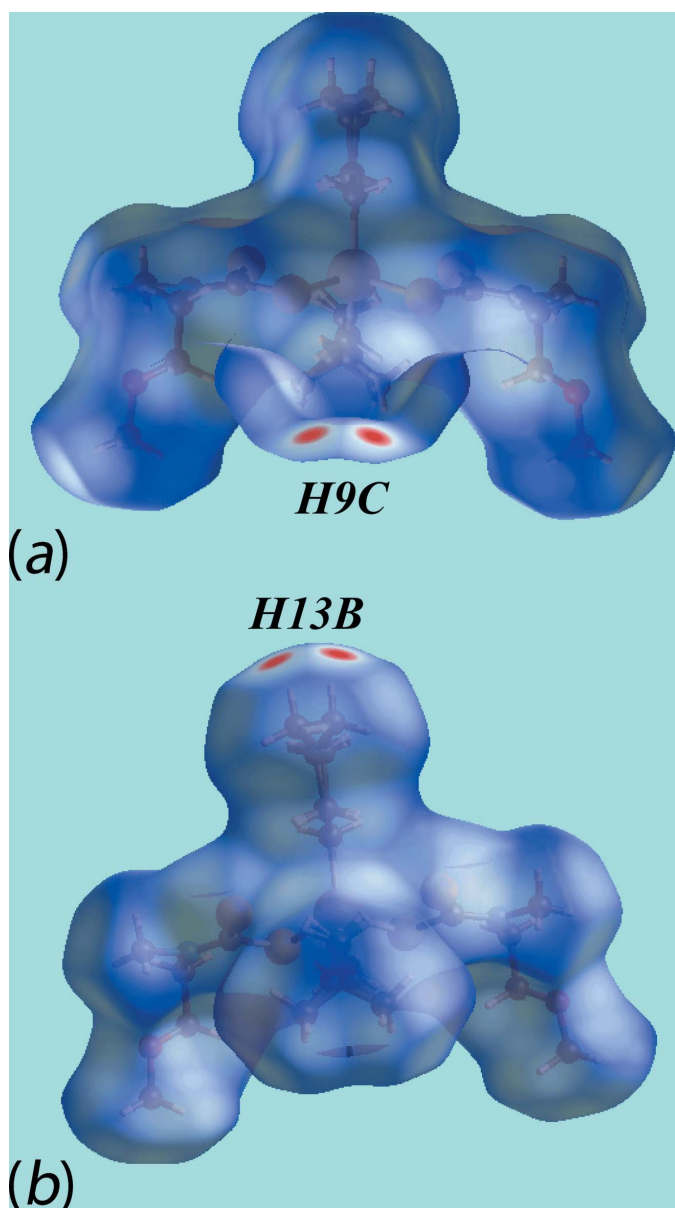


Figure 3
Two views of the Hirshfeld surface mapped over d_{norm} for (I). The disorder component has been retained in the images.

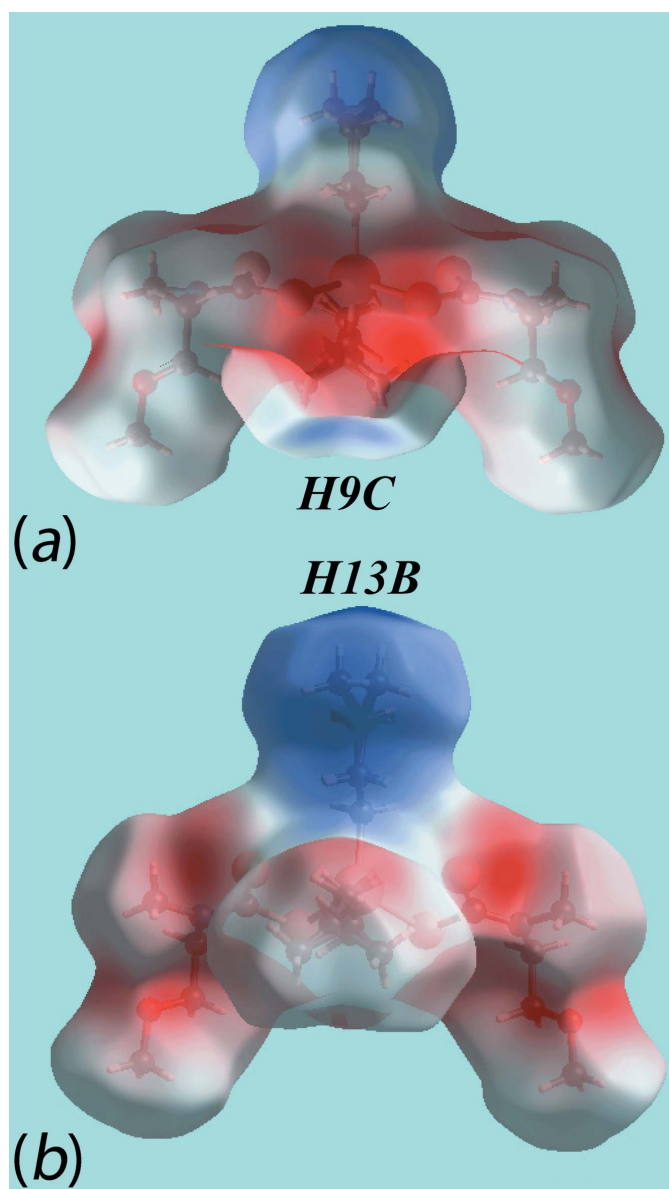


Figure 4
Two views of the Hirshfeld surfaces mapped over the electrostatic potential highlighting the disparate charge about the terminal hydrogen atoms (the red and blue regions represent negative and positive electrostatic potentials, respectively) for (I).

Table 3

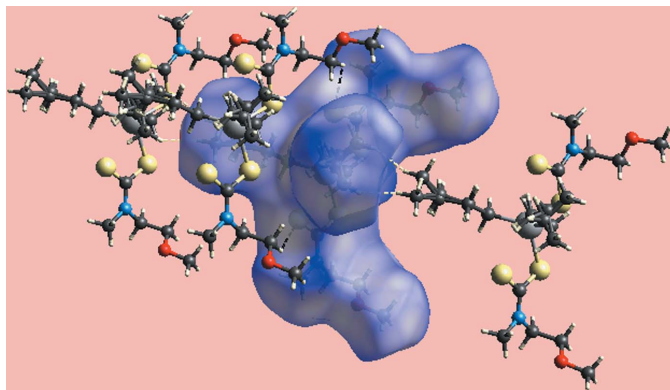
Percentage contribution of the different intermolecular contacts to the Hirshfeld surface in (I).

Contact	% contribution in (I)
H...H	74.5
S...H/H...S	16.2
O...H/H...O	4.9
C...H/H...C	3.2
N...H/H...N	1.2

highlighting the intermolecular C—H...S and H...H interactions.

From the overall two dimensional fingerprint plot, Fig. 6a, and those delineated (McKinnon *et al.*, 2007) into H...H, C...H/H...C, S...H/H...S, O...H/H...O and N...H/H...N contacts, illustrated in Fig. 6b–f, it is interesting to note that each of the specified interatomic contacts involves the participation of H atoms to the Hirshfeld surfaces. The quantitative summary showing the relative contributions from all interatomic contacts, given in Table 3, reinforces this fact.

In the fingerprint plot delineated into H...H contacts, Fig. 6b, a long and distinctive spike at $d_e + d_i \sim 1.8$ Å represents H...H bonding described above, Table 4, *i.e.* between methyl-H9B and -H13B atoms. The major contribution from these contacts to the Hirshfeld surface, *i.e.* 74.5%, and the essentially same shape of overall and H...H delineated fingerprint plots in the upper (d_e, d_i) region, Fig. 6a and b, show the dominance of these interactions in the molecular packing. The peak in the plot corresponding to a second short interatomic H...H contact, *i.e.* between methyl-H2B and methylene-H10A, Table 4, is diminished within the plot due to H9B...H13B interaction. The dihydrogen H...H bonding also results in short interatomic C...H/H...C contacts, Table 4, leading to a pair of short peaks at $d_e + d_i \sim 2.8$ Å in the delineated fingerprint plot, Fig. 6c; the other interatomic short C...H/H...C contact is merged within the plot. The presence of the weak C—H...S interactions, Table 2, is seen from the fingerprint plot corresponding to S...H/H...S contacts,


Figure 5

A view of the Hirshfeld surface mapped over d_{norm} for a reference molecule in contact with nearest neighbouring molecules and highlighting intermolecular C—H...S and H...H interactions, shown as white and black dashed lines, respectively.

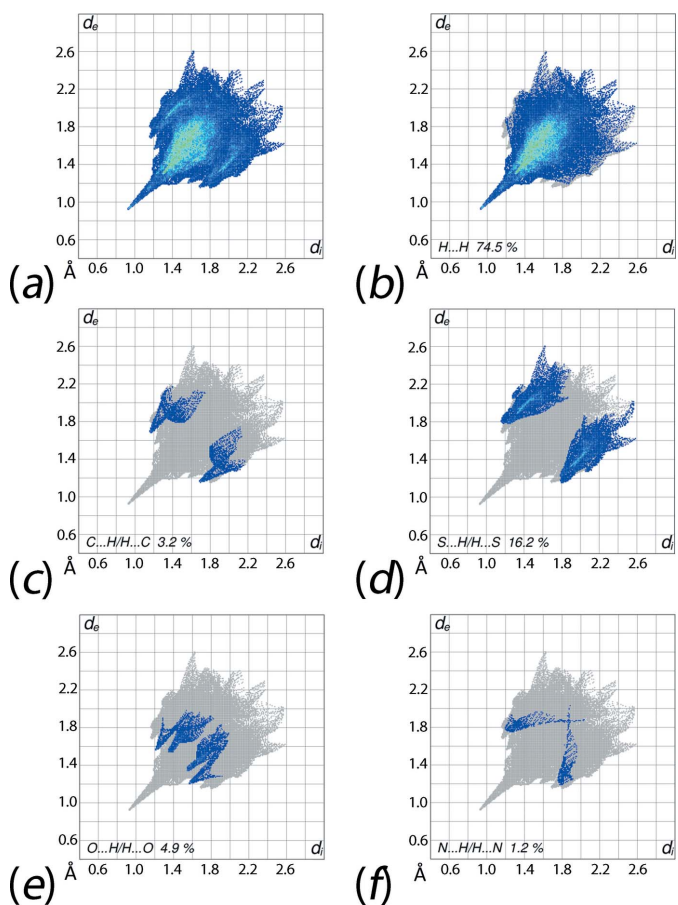
Table 4

Short interatomic contacts in (I).

Contact	distance	symmetry operation
H9C...H13B	1.85	$x, y, 1 + z$
H2B...H10A	2.27	$1 - x, -y, 1 - z$
C9...H13B	2.72	$x, y, 1 + z$
C13...H9C	2.73	$x, y, -1 + z$
C1...H2A	2.86	$1 - x, -y, 1 - z$
S2...H4B	2.96	$1 + x, y, z$

Fig. 6d, and is evident as a pair of broad peaks at $d_e + d_i \sim 2.9$ Å. The fingerprint plots delineated into O...H/H...O and N...H/H...N contacts, Fig. 6e and f, contribute in a minor fashion to the Hirshfeld surface and their characteristic points are longer than their respective van der Waals separations, *i.e.* longer than 2.72 and 2.75 Å, respectively, and hence it is likely they do not make any significant contribution to the molecular packing.

A comment on the relationship of the modelled disorder, the contribution of H...H contacts to the Hirshfeld surface and the nature of the H...H contacts is warranted. In the statistical disorder model for (I), it might be normally assumed


Figure 6

Views of the (a) full two-dimensional fingerprint plot for (I), and plots delineated into (b) H...H, (c) C...H/H...C, (d) S...H/H...S, (e) O...H/H...O and (f) N...H/H...N contacts.

(as done in Fig. 2*b*) that that H atoms adopt positions as far apart from each other as possible rather than participate in ‘non-bonded steric repulsion’ (Matta *et al.*, 2003). In (I), this does not appear to be the case but, rather is an example where H···H contacts contribute to the stabilization of the molecular packing. In examples where dihydrogen H···H contacts are formed intramolecularly, energies of stabilization up to 10 kcal mol⁻¹ have been suggested (Matta *et al.*, 2003).

4. Database survey

The interest in organotin dithiocarbamates is reflected in the relatively large number of crystal structures available in the crystallographic literature (Groom *et al.*, 2016). An example of this interest is twenty structures conforming to the general formula *n*-Bu₂Sn(S₂CNRR')₂. One structure, *i.e.* *R* = *R*' = *i*-Pr (Farina *et al.*, 2000), conforms to crystallographic *mm*2 symmetry (implying disorder in the terminal residues), seven, *i.e.* *R* = Me, *R*' = *n*-Bu (Ramasamy *et al.*, 2013), *R* = Me, *R*' = CH₂C(H)Me₂ (Ferreira *et al.*, 2012), *R* = Me, *R*' = methylene-1,3-dioxolan-2-yl (Ferreira *et al.*, 2012), *R* = Et, *R*' = methylene-4-pyridyl (Barba *et al.*, 2012), NR*R*' = piperidine (Khan *et al.*, 2015), NRR' = morpholine (Vrábel & Kellö, 1993) and NRR' = 4-(2-methoxyphenyl)piperazine (Zia-ur-Rehman *et al.*, 2012), have twofold symmetry with the remainder having no crystallographically imposed symmetry. This implies the structure of (I) is the first of this type to have crystallographic *m* symmetry. Two structures, *i.e.* *R* = *R*' = Et (Vrábel *et al.*, 1992) and *R* = *R*' = *n*-Bu (Ramasamy *et al.*, 2013), have two independent molecules in the crystallographic unit and, remarkably, one, *i.e.* *R* = *i*-Pr and *R*' = benzyl (Awang, Baba, Yousof *et al.*, 2010), has *Z*' = 5. In all, there are 26 independent dithiocarbamate ligands in *n*-Bu₂Sn(S₂CNRR')₂.

The first noteworthy comment to be made on the structures of *n*-Bu₂Sn(S₂CNRR')₂ is that they all conform to the same structural motif as adopted for (I). The Sn–S_{short} bond lengths in these structures span a relatively narrow range of 2.51 to 2.55 Å and cluster around 2.53 Å. As might be anticipated, a wider range is exhibited by the Sn–S_{long} bonds, *i.e.* 2.83 to 3.08 Å and these cluster around 2.96 Å. Given the range of Sn–S_{short} bond lengths is 0.04 Å and that for Sn–S_{long} is 0.25 Å, the observation that differences between the average values of Sn–S_{short} and Sn–S_{long} span a range of 0.43 Å indicates no specific correlations exist between Sn–S_{short} and Sn–S_{long} bond lengths. The S_{short}–Sn–S_{short}, S_{long}–Sn–S_{long} and C–Sn–C angles cluster around 83, 147 and 136°, respectively. However, these angles span ranges of 8° (range: 80 to 88°), 10° (140 to 151°) and 18° (127 to 145°), respectively. The disparity in the S–Sn–S angles is as expected from the adopted coordination geometry. While, generally, the S_{long}–Sn–S_{long} angles are wider than the C–Sn–C angles, there are three exceptional structures, namely *R* = *R*' = Et (Vrábel *et al.*, 1992), *R* = Et and *R*' = Cy (Awang, Baba, Yamin *et al.*, 2010) and *R* = benzyl and *R*' = methylene-4-pyridyl (Gupta *et al.*, 2015) have C–Sn–C which are marginally wider, by ca 1, than the S_{long}–Sn–S_{long} angles. The fact of non-systematic variations in the geometric parameters in organotin dithio-

Table 5
Experimental details.

Crystal data	
Chemical formula	[Sn(C ₄ H ₉) ₂ (C ₅ H ₁₀ NOS ₂) ₂]
<i>M_r</i>	561.43
Crystal system, space group	Monoclinic, <i>P</i> ₂ ₁ / <i>m</i>
Temperature (K)	148
<i>a</i> , <i>b</i> , <i>c</i> (Å)	7.1021 (4), 18.0761 (8), 10.8809 (7)
β (°)	108.877 (7)
<i>V</i> (Å ³)	1321.74 (14)
<i>Z</i>	2
Radiation type	Mo <i>K</i> α
μ (mm ⁻¹)	1.30
Crystal size (mm)	0.50 × 0.42 × 0.40
Data collection	
Diffractometer	Agilent Technologies SuperNova Dual diffractometer with an Atlas detector
Absorption correction	Multi-scan (<i>CrysAlis PRO</i> ; Agilent, 2015)
<i>T</i> _{min} , <i>T</i> _{max}	0.482, 1.000
No. of measured, independent and observed [<i>I</i> > 2σ(<i>I</i>)] reflections	10631, 4063, 3712
<i>R</i> _{int}	0.022
(sin θ/λ) _{max} (Å ⁻¹)	0.739
Refinement	
<i>R</i> [<i>F</i> ² > 2σ(<i>F</i> ²)], <i>wR</i> (<i>F</i> ²), <i>S</i>	0.027, 0.072, 1.12
No. of reflections	4063
No. of parameters	147
No. of restraints	2
H-atom treatment	H-atom parameters constrained
Δρ _{max} , Δρ _{min} (e Å ⁻³)	0.68, -0.56

Computer programs: *CrysAlis PRO* (Agilent, 2015), *SHELXL97* (Sheldrick, 2008), *SHELXL2014* (Sheldrick, 2015), *ORTEP-3 for Windows* (Farrugia, 2012), *DIAMOND* (Brandenburg, 2006) and *pubCIF* (Westrip, 2010).

carbamates has been commented upon previously (Buntine *et al.*, 1998; Muthalib *et al.*, 2014).

The homogeneity in the *n*-Bu₂Sn(S₂CNRR')₂ structural motif does not translate to the diphenyl analogues, *i.e.* Ph₂Sn(S₂CNRR')₂. Of the 19 structures conforming to this general formula, seven resemble the skew trapezoidal bipyramidal motif with the majority, *i.e.* twelve, having a *cis*-disposition of the tin-bound phenyl substituents. In this context, it is noteworthy that all structures of the general formula Sn(S₂CNRR')₂X₂, where *X* = halide, are invariably *cis*-S₄X₂ octahedral (Tiekink, 2008). Given the electronegativity of a phenyl group is intermediate between that of an alkyl group and a halide, it seems that there is a fine balance between adopting one structural motif over the other for Ph₂Sn(S₂CNRR')₂ compounds.

5. Synthesis and crystallization

(2-Methoxyethyl)methylamine (10 mmol) dissolved in ethanol (30 ml) was stirred in an ice bath (*ca* 277 K) for 30 min. 25% Ammonia solution (*ca* 2 ml) was added to make the solution basic. Then, a cold ethanol solution of carbon disulfide (10 mmol) was added to the solution followed by stirring for about 2 h. Next, di-*n*-butyltin(IV) dichloride (5 mmol), dissolved in ethanol (30 ml), was added to the solution which was further stirred for 2 h. The precipitate that formed was

filtered and then washed three times with cold ethanol to remove any impurities. The precipitate was then dried in a dessicator. The compound was crystallized in a mixture of chloroform and ethanol (1:2 v/v) at room temperature to give colourless slabs. Yield: 66%, m.p. 333–336 K. Analysis. Found C, 40.3; H, 7.3; N, 5.0; S, 22.8. $C_{18}H_{38}N_2O_2S_4Sn$ requires: C, 38.5; H, 6.8; N, 5.0; S, 23.7. IR (cm^{-1}): 1490 $\nu(C-N)$, 991 $\nu(C-S)$, 553 $\nu(Sn-C)$, 420 $\nu(Sn-S)$. 1H NMR ($CDCl_3$): 7.40–7.74 (15H, Sn–Ph), 4.07 (2H, OCH_2), 3.71 (2H, NCH_2), 3.46 (3H, OCH_3), 3.40 (3H, NCH_3), 2.04 (2H, $SnCH_2$), 1.92 (2H, $SNCH_2CH_2$), 1.44 (2H, CH_2CH_3), 0.98 (3H, CH_2CH_3). $^{13}C\{^1H\}$ NMR ($CDCl_3$): δ 201.2 (S_2C), 70.1 (OCH_2), 59.1 (NCH_2), 56.6 (OCH_3), 44.5 (NCH_3), 34.3 ($SnCH_2$), 28.6 ($SnCH_2CH_2$), 26.5 (CH_2CH_3), 13.9 (CH_2CH_3). $^{119}Sn\{^1H\}$ NMR ($CDCl_3$): 338.6.

6. Refinement

Crystal data, data collection and structure refinement details are summarized in Table 5. Carbon-bound H atoms were placed in calculated positions ($C-H = 0.98-0.99 \text{ \AA}$) and were included in the refinement in the riding model approximation, with $U_{iso}(H)$ set to $1.2-1.5U_{eq}(C)$. The molecule has crystallographic mirror symmetry with the Sn atom and *n*-butyl-C atoms lying on the plane. The terminal CH_2CH_3 residue of each *n*-butyl group is statistically disordered across this plane. Owing to poor agreement, three reflections, *i.e.* (172), (124) and (155), were omitted from the final cycles of refinement.

Acknowledgements

This work was supported by grant GGPM-2016-061. We gratefully acknowledge the School of Chemical Science and Food Technology, Universiti Kebangsaan Malaysia for providing the essential laboratory facilities. We would also like to acknowledge the technical support from the laboratory assistants of the Faculty of Science and Technology, Universiti Kebangsaan Malaysia. Intensity data were collected in the University of Malaya crystallographic laboratory.

Funding information

Funding for this research was provided by: Universiti Kebangsaan Malaysia (award No. GGPM-2016-061).

References

Agilent (2015). *CrysAlis PRO*. Agilent Technologies Inc., Santa Clara, CA, USA.

- Awang, N., Baba, I., Yousof, N. S. A. M. & Kamaludin, N. F. (2010). *Am. J. Appl. Sci.* **7**, 1047–1052.
- Awang, N., Baba, I., Yamin, B. M. & Ng, S. W. (2010). *Acta Cryst.* **E66**, m938.
- Barba, V., Arenaza, B., Guerrero, J. & Reyes, R. (2012). *Heteroat. Chem.* **23**, 422–428.
- Brandenburg, K. (2006). *DIAMOND*. Crystal Impact GbR, Bonn, Germany.
- Buntine, M. A., Hall, V. J., Kosovel, F. J. & Tiekink, E. R. T. (1998). *J. Phys. Chem. A*, **102**, 2472–2482.
- Farina, Y., Baba, I., Othman, A. H. & Ng, S. W. (2000). *Main Group Met. Chem.* **23**, 795–796.
- Farrugia, L. J. (2012). *J. Appl. Cryst.* **45**, 849–854.
- Ferreira, I. P., de Lima, G. M., Paniago, E. B., Rocha, W. R., Takahashi, J. A., Pinheiro, C. B. & Ardisson, J. D. (2012). *Eur. J. Med. Chem.* **58**, 493–503.
- Ferreira, I. P., de Lima, G. M., Paniago, E. B., Rocha, W. R., Takahashi, J. A., Pinheiro, C. B. & Ardisson, J. D. (2014). *Polyhedron*, **79**, 161–169.
- Groom, C. R., Bruno, I. J., Lightfoot, M. P. & Ward, S. C. (2016). *Acta Cryst.* **B72**, 171–179.
- Gupta, A. N., Kumar, V., Singh, V., Rajput, A., Prasad, L. B., Drew, M. G. B. & Singh, N. (2015). *J. Organomet. Chem.* **787**, 65–72.
- Kadu, R., Roy, H. & Singh, V. K. (2015). *Appl. Organomet. Chem.* **29**, 746–755.
- Khan, M. D., Akhtar, J., Malik, M. A., Akhtar, M. & Revaprasadu, N. (2015). *New J. Chem.* **39**, 9569–9574.
- Khan, N., Farina, Y., Mun, L. K., Rajab, N. F. & Awang, N. (2014). *J. Mol. Struct.* **1076**, 403–410.
- Kim, K., Ibers, J. A., Jung, O.-S. & Sohn, Y. S. (1987). *Acta Cryst.* **C43**, 2317–2319.
- Matta, C. F., Hernández-Trujillo, J., Tang, T.-H. & Bader, R. F. W. (2003). *Chem. Eur. J.* pp. 1940–1951.
- McKinnon, J. J., Jayatilaka, D. & Spackman, M. A. (2007). *Chem. Commun.* pp. 3814–3816.
- Mohamad, R., Awang, N., Jotani, M. M. & Tiekink, E. R. T. (2016). *Acta Cryst.* **E72**, 1130–1137.
- Mohamad, R., Awang, N., Kamaludin, N. F., Jotani, M. M. & Tiekink, E. R. T. (2016). *Acta Cryst.* **E72**, 1480–1487.
- Muthalib, A. F. A., Baba, I., Khaledi, H., Ali, H. M. & Tiekink, E. R. T. (2014). *Z. Kristallogr.* **229**, 39–46.
- Ng, S. W., Wei, C., Kumar Das, V. G., Jameson, G. B. & Butcher, R. J. (1989). *J. Organomet. Chem.* **365**, 75–82.
- Ramasamy, K., Kuznetsov, V. L., Gopal, K., Malik, M. A., Raftery, J., Edwards, P. P. & O'Brien, P. (2013). *Chem. Mater.* **25**, 266–276.
- Sheldrick, G. M. (2008). *Acta Cryst.* **A64**, 112–122.
- Sheldrick, G. M. (2015). *Acta Cryst.* **C71**, 3–8.
- Tiekink, E. R. T. (2008). *Appl. Organomet. Chem.* **22**, 533–550.
- Vrábel, V. & Kellö, E. (1993). *Acta Cryst.* **C49**, 873–875.
- Vrábel, V., Lokaj, J., Kellö, E., Garaj, J., Batsanov, A. C. & Struchkov, Yu. T. (1992). *Acta Cryst.* **C48**, 633–635.
- Westrip, S. P. (2010). *J. Appl. Cryst.* **43**, 920–925.
- Yu, Y., Yang, H., Wei, Z.-W. & Tang, L.-F. (2014). *Heteroat. Chem.* **25**, 274–281.
- Zia-ur-Rehman, Muhammad, N., Shah, A., Ali, S., Butler, I. S. & Meetsma, A. (2012). *J. Coord. Chem.* **65**, 3238–3253.

supporting information

Acta Cryst. (2017). E73, 260-265 [https://doi.org/10.1107/S2056989017001098]

Di-*n*-butylbis[*N*-(2-methoxyethyl)-*N*-methyldithiocarbamato- κ^2 S,S']tin(IV): crystal structure and Hirshfeld surface analysis

Rapidah Mohamad, Normah Awang, Nurul F. Kamaludin, Mukesh M. Jotani and Edward R. T. Tiekink

Computing details

Data collection: *CrysAlis PRO* (Agilent, 2015); cell refinement: *CrysAlis PRO* (Agilent, 2015); data reduction: *CrysAlis PRO* (Agilent, 2015); program(s) used to solve structure: *SHELXL97* (Sheldrick, 2008); program(s) used to refine structure: *SHELXL2014* (Sheldrick, 2015); molecular graphics: *ORTEP-3 for Windows* (Farrugia, 2012) and *DIAMOND* (Brandenburg, 2006); software used to prepare material for publication: *publCIF* (Westrip, 2010).

Di-*n*-butylbis[*N*-(2-methoxyethyl)-*N*-methyldithiocarbamato- κ^2 S,S']tin(IV)

Crystal data

[Sn(C₄H₉)₂(C₅H₁₀NOS₂)₂]

$M_r = 561.43$

Monoclinic, $P2_1/m$

$a = 7.1021$ (4) Å

$b = 18.0761$ (8) Å

$c = 10.8809$ (7) Å

$\beta = 108.877$ (7)°

$V = 1321.74$ (14) Å³

$Z = 2$

$F(000) = 580$

$D_x = 1.411$ Mg m⁻³

Mo $K\alpha$ radiation, $\lambda = 0.71073$ Å

Cell parameters from 6472 reflections

$\theta = 4.5$ – 31.4 °

$\mu = 1.30$ mm⁻¹

$T = 148$ K

Block, colourless

$0.50 \times 0.42 \times 0.40$ mm

Data collection

Agilent Technologies SuperNova Dual
diffractometer with an Atlas detector
Radiation source: SuperNova (Mo) X-ray
Source

Mirror monochromator

Detector resolution: 10.4041 pixels mm⁻¹

ω scan

Absorption correction: multi-scan
(*CrysAlis PRO*; Agilent, 2015)

$T_{\min} = 0.482$, $T_{\max} = 1.000$

10631 measured reflections

4063 independent reflections

3712 reflections with $I > 2\sigma(I)$

$R_{\text{int}} = 0.022$

$\theta_{\max} = 31.7$ °, $\theta_{\min} = 3.8$ °

$h = -6 \rightarrow 10$

$k = -26 \rightarrow 25$

$l = -15 \rightarrow 12$

Refinement

Refinement on F^2

Least-squares matrix: full

$R[F^2 > 2\sigma(F^2)] = 0.027$

$wR(F^2) = 0.072$

$S = 1.12$

4063 reflections

147 parameters

2 restraints

Hydrogen site location: inferred from
neighbouring sites

H-atom parameters constrained

$w = 1/[\sigma^2(F_o^2) + (0.0308P)^2 + 0.5383P]$

where $P = (F_o^2 + 2F_c^2)/3$

$(\Delta/\sigma)_{\max} = 0.002$

$\Delta\rho_{\max} = 0.68$ e Å⁻³

$\Delta\rho_{\min} = -0.56$ e Å⁻³

Special details

Geometry. All esds (except the esd in the dihedral angle between two l.s. planes) are estimated using the full covariance matrix. The cell esds are taken into account individually in the estimation of esds in distances, angles and torsion angles; correlations between esds in cell parameters are only used when they are defined by crystal symmetry. An approximate (isotropic) treatment of cell esds is used for estimating esds involving l.s. planes.

Fractional atomic coordinates and isotropic or equivalent isotropic displacement parameters (\AA^2)

	<i>x</i>	<i>y</i>	<i>z</i>	$U_{\text{iso}}^*/U_{\text{eq}}$	Occ. (<1)
Sn	0.63209 (3)	0.2500	0.65708 (2)	0.02489 (6)	
S1	0.36767 (7)	0.15500 (2)	0.65625 (5)	0.02861 (11)	
S2	0.76229 (7)	0.09574 (3)	0.66305 (5)	0.02966 (11)	
O1	0.3352 (2)	-0.06447 (9)	0.86623 (16)	0.0396 (3)	
N1	0.4586 (2)	0.01192 (8)	0.66892 (16)	0.0266 (3)	
C1	0.5266 (3)	0.08039 (10)	0.66318 (17)	0.0234 (3)	
C2	0.5918 (3)	-0.05193 (11)	0.6850 (2)	0.0341 (4)	
H2A	0.6388	-0.0555	0.6099	0.051*	
H2B	0.5197	-0.0972	0.6916	0.051*	
H2C	0.7059	-0.0458	0.7642	0.051*	
C3	0.2511 (3)	-0.00359 (11)	0.6614 (2)	0.0298 (4)	
H3A	0.2103	-0.0516	0.6170	0.036*	
H3B	0.1637	0.0351	0.6080	0.036*	
C4	0.2207 (3)	-0.00634 (11)	0.7922 (2)	0.0325 (4)	
H4A	0.2615	0.0413	0.8380	0.039*	
H4B	0.0781	-0.0144	0.7807	0.039*	
C5	0.2984 (4)	-0.07280 (17)	0.9863 (3)	0.0531 (7)	
H5A	0.3355	-0.0272	1.0371	0.080*	
H5B	0.3776	-0.1141	1.0350	0.080*	
H5C	0.1568	-0.0829	0.9697	0.080*	
C6	0.8488 (4)	0.2500	0.8477 (3)	0.0309 (6)	
H6A	0.8300	0.2943	0.8959	0.037*	0.5
H6B	0.8300	0.2057	0.8959	0.037*	0.5
C7	1.0587 (5)	0.2500	0.8393 (3)	0.0453 (8)	
H7A	1.0830	0.2982	0.8039	0.054*	0.5
H7B	1.0677	0.2111	0.7773	0.054*	0.5
C8	1.2246 (7)	0.2366 (3)	0.9707 (5)	0.0471 (18)	0.5
H8A	1.1858	0.1960	1.0186	0.056*	0.5
H8B	1.3502	0.2226	0.9557	0.056*	0.5
C9	1.2526 (10)	0.3068 (4)	1.0476 (7)	0.0674 (16)*	0.5
H9A	1.2572	0.3488	0.9916	0.101*	0.5
H9B	1.3776	0.3043	1.1202	0.101*	0.5
H9C	1.1413	0.3133	1.0813	0.101*	0.5
C10	0.6376 (4)	0.2500	0.4618 (3)	0.0278 (5)	
H10A	0.5652	0.2058	0.4167	0.033*	0.5
H10B	0.5652	0.2942	0.4167	0.033*	0.5
C11	0.8436 (5)	0.2500	0.4497 (3)	0.0442 (8)	
H11A	0.9132	0.2039	0.4883	0.053*	0.5
H11B	0.9200	0.2923	0.4994	0.053*	0.5

C12	0.8384 (7)	0.2556 (15)	0.3070 (4)	0.059 (3)	0.5
H12A	0.7967	0.2074	0.2637	0.071*	0.5
H12B	0.7378	0.2929	0.2615	0.071*	0.5
C13	1.0384 (9)	0.2771 (5)	0.2943 (6)	0.086 (3)	0.5
H13A	1.0801	0.3251	0.3361	0.129*	0.5
H13B	1.0263	0.2805	0.2021	0.129*	0.5
H13C	1.1378	0.2395	0.3364	0.129*	0.5

Atomic displacement parameters (Å²)

	U^{11}	U^{22}	U^{33}	U^{12}	U^{13}	U^{23}
Sn	0.02457 (10)	0.02545 (9)	0.02660 (10)	0.000	0.01098 (7)	0.000
S1	0.0263 (2)	0.0217 (2)	0.0407 (3)	0.00326 (16)	0.0147 (2)	0.00337 (18)
S2	0.0279 (2)	0.0278 (2)	0.0364 (3)	0.00582 (17)	0.0146 (2)	0.00320 (18)
O1	0.0414 (8)	0.0371 (8)	0.0389 (9)	0.0048 (6)	0.0112 (7)	0.0136 (7)
N1	0.0304 (8)	0.0225 (7)	0.0267 (8)	0.0017 (6)	0.0091 (7)	-0.0005 (6)
C1	0.0269 (8)	0.0243 (8)	0.0194 (8)	0.0017 (6)	0.0080 (7)	-0.0005 (6)
C2	0.0412 (11)	0.0221 (8)	0.0390 (11)	0.0061 (8)	0.0132 (9)	-0.0005 (8)
C3	0.0290 (9)	0.0254 (8)	0.0314 (10)	-0.0022 (7)	0.0048 (8)	0.0023 (7)
C4	0.0303 (9)	0.0318 (9)	0.0358 (11)	0.0016 (7)	0.0113 (8)	0.0071 (8)
C5	0.0475 (14)	0.0690 (17)	0.0420 (14)	-0.0079 (12)	0.0134 (11)	0.0210 (12)
C6	0.0325 (14)	0.0377 (14)	0.0241 (13)	0.000	0.0115 (11)	0.000
C7	0.0279 (14)	0.074 (2)	0.0311 (16)	0.000	0.0051 (13)	0.000
C8	0.044 (2)	0.045 (6)	0.043 (2)	0.003 (2)	0.0020 (18)	0.001 (2)
C10	0.0330 (13)	0.0241 (11)	0.0263 (13)	0.000	0.0096 (11)	0.000
C11	0.0391 (17)	0.066 (2)	0.0323 (17)	0.000	0.0185 (14)	0.000
C12	0.059 (2)	0.091 (8)	0.0343 (19)	0.021 (7)	0.0253 (19)	-0.006 (6)
C13	0.070 (4)	0.148 (10)	0.061 (4)	-0.013 (4)	0.048 (3)	-0.011 (4)

Geometric parameters (Å, °)

Sn—S1	2.5425 (5)	C6—C7	1.523 (4)
Sn—S2	2.9318 (5)	C6—H6A	0.9900
Sn—S1 ⁱ	2.5425 (5)	C6—H6B	0.9900
Sn—S2 ⁱ	2.9318 (5)	C7—C8	1.550 (5)
Sn—C6	2.146 (3)	C7—H7A	0.9900
Sn—C10	2.138 (3)	C7—H7B	0.9900
S1—C1	1.7443 (18)	C8—C9	1.498 (7)
S2—C1	1.6974 (19)	C8—H8A	0.9900
O1—C4	1.411 (2)	C8—H8B	0.9900
O1—C5	1.421 (3)	C9—H9A	0.9800
N1—C1	1.337 (2)	C9—H9B	0.9800
N1—C2	1.466 (2)	C9—H9C	0.9800
N1—C3	1.476 (2)	C10—C11	1.511 (4)
C2—H2A	0.9800	C10—H10A	0.9900
C2—H2B	0.9800	C10—H10B	0.9900
C2—H2C	0.9800	C11—C12	1.545 (5)
C3—C4	1.508 (3)	C11—H11A	0.9900

C3—H3A	0.9900	C11—H11B	0.9900
C3—H3B	0.9900	C12—C13	1.521 (8)
C4—H4A	0.9900	C12—H12A	0.9900
C4—H4B	0.9900	C12—H12B	0.9900
C5—H5A	0.9800	C13—H13A	0.9800
C5—H5B	0.9800	C13—H13B	0.9800
C5—H5C	0.9800	C13—H13C	0.9800
C10—Sn—C6	136.27 (11)	C7—C6—H6B	109.5
C10—Sn—S1	104.32 (6)	Sn—C6—H6B	109.5
C6—Sn—S1	107.55 (5)	H6A—C6—H6B	108.1
C10—Sn—S1 ⁱ	104.32 (6)	C6—C7—C8	114.3 (3)
C6—Sn—S1 ⁱ	107.55 (5)	C6—C7—H7A	108.7
S1—Sn—S1 ⁱ	84.97 (2)	C8—C7—H7A	108.7
C10—Sn—S2	85.12 (2)	C6—C7—H7B	108.7
C6—Sn—S2	81.73 (2)	C8—C7—H7B	108.7
S1—Sn—S2	65.482 (14)	H7A—C7—H7B	107.6
S1 ⁱ —Sn—S2	150.431 (15)	C9—C8—C7	107.9 (4)
C1—S1—Sn	93.17 (6)	C9—C8—H8A	110.1
C1—S2—Sn	81.45 (6)	C7—C8—H8A	110.1
C4—O1—C5	111.11 (19)	C9—C8—H8B	110.1
C1—N1—C2	120.35 (16)	C7—C8—H8B	110.1
C1—N1—C3	122.84 (15)	H8A—C8—H8B	108.4
C2—N1—C3	116.80 (15)	C8—C9—H9A	109.5
N1—C1—S2	121.49 (14)	C8—C9—H9B	109.5
N1—C1—S1	118.64 (14)	H9A—C9—H9B	109.5
S2—C1—S1	119.87 (10)	C8—C9—H9C	109.5
N1—C2—H2A	109.5	H9A—C9—H9C	109.5
N1—C2—H2B	109.5	H9B—C9—H9C	109.5
H2A—C2—H2B	109.5	C11—C10—Sn	114.6 (2)
N1—C2—H2C	109.5	C11—C10—H10A	108.6
H2A—C2—H2C	109.5	Sn—C10—H10A	108.6
H2B—C2—H2C	109.5	C11—C10—H10B	108.6
N1—C3—C4	113.55 (16)	Sn—C10—H10B	108.6
N1—C3—H3A	108.9	H10A—C10—H10B	107.6
C4—C3—H3A	108.9	C10—C11—C12	112.3 (3)
N1—C3—H3B	108.9	C10—C11—H11A	109.2
C4—C3—H3B	108.9	C12—C11—H11A	109.2
H3A—C3—H3B	107.7	C10—C11—H11B	109.2
O1—C4—C3	109.33 (17)	C12—C11—H11B	109.2
O1—C4—H4A	109.8	H11A—C11—H11B	107.9
C3—C4—H4A	109.8	C13—C12—C11	112.9 (5)
O1—C4—H4B	109.8	C13—C12—H12A	109.0
C3—C4—H4B	109.8	C11—C12—H12A	109.0
H4A—C4—H4B	108.3	C13—C12—H12B	109.0
O1—C5—H5A	109.5	C11—C12—H12B	109.0
O1—C5—H5B	109.5	H12A—C12—H12B	107.8
H5A—C5—H5B	109.5	C12—C13—H13A	109.5

O1—C5—H5C	109.5	C12—C13—H13B	109.5
H5A—C5—H5C	109.5	H13A—C13—H13B	109.5
H5B—C5—H5C	109.5	C12—C13—H13C	109.5
C7—C6—Sn	110.60 (19)	H13A—C13—H13C	109.5
C7—C6—H6A	109.5	H13B—C13—H13C	109.5
Sn—C6—H6A	109.5		
C2—N1—C1—S2	4.5 (3)	C1—N1—C3—C4	-91.6 (2)
C3—N1—C1—S2	-176.29 (14)	C2—N1—C3—C4	87.6 (2)
C2—N1—C1—S1	-175.26 (14)	C5—O1—C4—C3	-175.28 (18)
C3—N1—C1—S1	3.9 (2)	N1—C3—C4—O1	-62.2 (2)
Sn—S2—C1—N1	-178.28 (16)	Sn—C6—C7—C8	-170.1 (2)
Sn—S2—C1—S1	1.51 (10)	C6—C7—C8—C9	-76.4 (5)
Sn—S1—C1—N1	178.07 (14)	Sn—C10—C11—C12	-175.9 (11)
Sn—S1—C1—S2	-1.72 (11)	C10—C11—C12—C13	164.0 (11)

Symmetry code: (i) $x, -y+1/2, z$.

Hydrogen-bond geometry (Å, °)

$D-H\cdots A$	$D-H$	$H\cdots A$	$D\cdots A$	$D-H\cdots A$
C4—H4B \cdots S2 ⁱⁱ	0.99	2.96	3.608 (2)	124

Symmetry code: (ii) $x-1, y, z$.